# Distance Determination of RR Lyrae Stars AE Leo, AT Vir, and HY Com

**Cody Soper**
**Christopher Tenenbaum**
**Adam Lounsbery**
**Jarred Rheiner**
**David Klassen** (ORCID 0000-0001-6142-1982)
*Department of Physics and Astronomy, Rowan University, Glassboro, NJ; soperc46@students.rowan.edu*

*Received June 21, 2021; revised April 11, 2022; accepted April 19, 2022*

**Abstract** We present the results of our observations and analyses of three RR Lyrae variable stars: AT Vir, HY Com, and AE Leo, in order to test period-luminosity relationships derived from stellar models. We have measured the periods of these stars to be 0.52359, 0.44898, and 0.63021 days, respectively, closely matching previous work. Period-Luminosity-Metallicity (PLM) relationships were used to calculate new distance values which averaged 1331 ± 41 pc, 957 ± 49 pc, and 2480 ± 76 pc for AT Vir, HY Com, and AE Leo, respectively. These measurements are compared with Gaia distances calculated from EDR3 parallax angles. Our results appear to generally support the PLM relationship with distance differences less than 2σ.

## 1. Introduction

RR Lyrae stars are low–mass, horizontal branch, pulsating variable stars with periods of less than a day. Longmore *et al.* (1986) observed that there exist period-luminosity (PL) relationships that can allow us to measure the distance to globular clusters where these stars are known to exist. However, a relation was only found in the K band. Later, work by Catelan *et al.* (2004) established theoretical relations for the absolute magnitudes in I, J, H, K, and V, and later Cáceres and Catelan (2008) established further theoretical relations in i' and z. Confirmation of these relations can help in the general overall understanding of RR Lyrae stars.

In our study, observations of known RR Lyrae stars AT Vir, HY Com, and AE Leo are made in B, V , i', and z filters over several periods. From here we use the established period-luminosity relations and metallicities of our stars found in the literature to calculate their distances. Our goal is to compare these results to Gaia parallax distance measurements and test the P-L relations.

## 2. Observations and methods

Our three observed stars, AT Vir, HY Com, and AE Leo, were chosen from a list of RR Lyrae variable stars whose distance has been measured by Gaia and was provided by the Our Solar Siblings project team (OSS) (Fitzgerald *et al.* 2018). Through the OSS, we received access to Las Cumbres Observatories' (LCO) (Brown *et al.* 2013) international system of 0.4-meter robotic telescopes. With these telescopes, Images of our stars were collected in B, V , i', and z filters.

As these stars are short period variables, and we want to collect images robotically over time, we first collected test images for each of them with estimated exposure times and then used the aperture tool in AstroImageJ (Collins *et al.* 2017) to ensure counts would be within an acceptable range (source−sky of 10–500 thousand counts) that would neither saturate the frame nor be so faint as to have low signal-to-noise. These final exposure times used for our observations are presented in Table 1.

Table 1. Filters and exposure times used.

| *Filter* | *λ (Å)* | *Δλ (Å)* | *Exposure Time (s)* *AT Vir* | *HY Com* | *AE Leo* |
|---|---|---|---|---|---|
| B | 4361 | 890 | 30 | 20 | 36 |
| V | 5448 | 840 | 30 | 20 | 36 |
| i' | 7540 | 1290 | 30 | 20 | 36 |
| z | 8700 | 1040 | 90 | 45 | 60 |

Once viable exposure times were found, we scheduled 84 observations in B, V , i', and z filters for each of our three stars, with images requested every 3 hours. As these stars all should have periods of less than a day, this cadence should ensure good coverage for several periods Of these 84 scheduled observations, 66 were successful; some were lost due to weather or scheduling clashes with other programs. The collected images were then processed through the OSS Pipeline (Fitzgerald 2018), which reduces cosmic rays, standardizes file names, and performs six different photometric measurements on all stars in the frame. For our purposes, we were able to obtain reliable results using the Source Extractor (SExtractor) photometry method (Bertin and Arnouts 1996) and therefore this was the only method of the six that we used. The SExtractor method is an automated process that makes a catalog of all of the stars in a given image after analyzing the image by estimating the background, thresholding, deblending, filtering, photometry on each source, and finally separating stars/galaxies.

The resulting photometry files were processed using the Astrosource package (Fitzgerald *et al.* 2021) to calculate phased light curves as well as average magnitudes, amplitudes, and periods for our observed stars. Calibration of our comparison stars were done by crossmatching to the APASS catalog (Henden *et al.* 2016) for B and V filters, and Skymapper DR1.1 (Wolf *et al.* 2018) for i' and z filters. The package does this by means of the Phase Dispersion Minimization (PDM)

method (Stellingwerf 1978), which uses a least–squares fitting technique that seeks to minimize the dispersion of the data from our images at constant phase, and String Length (SL) method (Lafler and Kinman 1965), which is another least–squares approach that uses trial periods to calculate the best fit for the period. Other needed information, such as interstellar reddening and metallicity, were found in the literature and used in tandem with our results from Astrosource to calculate the distance to our stars.

Metallicity, reported as [Fe/H], was converted to logZ for use in the period-luminosity relation. The metallicity of our stars was found using the VizieR catalog (Ochsenbein *et al.* 2000) for links to primary sources and tabulations of those results. The conversions were done using the equations presented by Catelan *et al.* (2004) and are reprinted here in Equations 1 and 2. They note that $f_\alpha = 10^{[\alpha/Fe]}$, a scaling factor to account for enhancement of α-elements (Salaris *et al.* 1993); it is assumed that $[\alpha/Fe] \approx 0.3$.

$$[M/H] = [Fe/H] + \log(0.638 f_\alpha + 0.362) \quad (1)$$

$$\log Z = [M/H] - 1.765 \quad (2)$$

The value from Equation 2 is then used in the PLM relations for the V , i', and z bands in Equations 3, 4, and 5 below. These equations were first theorized for V by Catelan *et al.* (2004), and then later for i' and z by Cáceres and Catelan (2008).

$$M_V = 2.288 + 0.882 \log Z + 0.108 (\log Z)^2 \quad (3)$$

$$M_i = 0.908 - 1.035 \log P + 0.220 \log Z \quad (4)$$

$$M_z = 0.839 - 1.295 \log P + 0.211 \log Z \quad (5)$$

When calculating the distance of our star, we also had to take into consideration the extinction factor due to interstellar dust for each star. Reddening values, E(B−V), found in the NASA/IPAC Infrared Science Archive (Desai *et al.* 2018) were originally calculated for our stars by Schlafly and Finkbeiner (2011). These were then be used to calculate the extinction, A, for each of our filters based on Cardelli *et al.* (1989) as shown in Equations 6, 7, and 8 below.

$$A_V = E[B-V] \times R \times 1 \quad (6)$$

$$A_i = E[B-V] \times R \times 0.68319 \quad (7)$$

$$A_z = E[B-V] \times R \times 0.49264 \quad (8)$$

where R = 3.1 is a standard value for the galaxy and $A_V$, $A_i$, and $A_z$ are the extinction corrections for the V, i', and z bands, respectively. The values of M and A for each of our filters can then finally be used with the average apparent magnitude, m, of our star calculated by Astrosource to obtain the distance of our star in parsecs, D, using:

$$D = 10^{(m-M-A+5)/5} \quad (9)$$

The distance calculated can then be compared to the distance measured by Gaia as reported in Gaia EDR3 (Gaia Collab. *et al.* 2021). Table 2 shows these Gaia distances and other general information discussed above for our selected stars.

## 3. Results

We present the results of our work in the tables and figures below. Table 2 gives basic information on each star found in the literature. Tables 3–8 and Figures 1–6 are the various results for each star in turn: AT Vir, HY Com, and AE Leo. We include: the plot for period likelihood (Figures 1, 3, 5), the phased light curves using the period with highest likelihood in each filter (Figures 2, 4, 6), the periods and "middle magnitudes" in each filter (Tables 3, 5, 7), and the calculated extinction, measured apparent magnitude, calculated absolute magnitude, and calculated distance in each filter (Tables 4, 6, 8).

Given that the period likelihood for each star is equivalent within uncertainty for all filters and across both methods, the period likelihood plot will only be presented for the i' filter using the PDM method for each of our stars as representative of our results and to save space. The center of the first peak is chosen as the most likely period.

Similarly, phased light curves for each of our stars will only be presented using the most likely period from the PDM method, as they are equivalent within uncertainty to curves produced by the SL method.

Note that "middle magnitude" is calculated as the average of the brightest and dimmest magnitude in the calibrated series and is not a mathematical mean over the entire set of measurements. Since we cannot be sure we have adequately sampled the possible brightness values, a standard mean could suffer from bias. By taking the middle value we avoid that.

The uncertainty errors on the light curves are due to the photometry process itself. They are strongly influenced by signal-to-noise (S/N) based on integration time, number of comparison field stars in the image, and potential drops in S/N due to variation in sky conditions with a fixed integration time across the observing period. As the observing requests for each of the three stars were done independently, sky conditions for any run of images can vary between them significantly.

Table 2. General information and Gaia distances.

| *Star* | *Type* | *R.A. (deg.)* | *Dec (deg.).* | *[Fe/H]* | *E(B−V)* | *$\bar{\omega}$ (mas)* |
|---|---|---|---|---|---|---|
| AT Vir | RRab | 193.7936 | −05.45923 | −1.87 ± 0.10 | 0.0314 ± 0.0012 | 0.7579 ± 0.0401 |
| HY Com | RRc | 98.73142 | −45.30863 | −1.75 ± 0.02 | 0.0237 ± 0.0004 | 0.9616 ± 0.0189 |
| AE Leo | RRab/bl | 171.55094 | 17.6609 | −1.71 ± 0.11 | 0.0200 ± 0.0009 | 0.3706 ± 0.0188 |

*Note: Metallicities for AT Vir and HY Com are from Crestani* et al. *(2021), and AE Leo is from Layden (1994). Error for AT Vir was set to a standard value by the authors due to an insufficient number of measurements to calculate it. Gaia parallax angles from EDR3 (Gaia Collaboration* et al. *2021) reported at VizieR.*

Table 3. Calculated period, middle magnitude, and amplitude of AT Vir.

| | *Period Calculations* | | | |
|---|---|---|---|---|
| *Filter* | *PDM* | *SL* | *Middle Magnitude* | *Amplitude* |
| B | 0.5065 ± 0.0069 | 0.5254 ± 0.009 | 11.471 ± 0.071 | 1.673 |
| V | 0.5254 ± 0.0058 | 0.5254 ± 0.0069 | 11.266 ± 0.106 | 1.322 |
| i' | 0.5263 ± 0.0115 | 0.5254 ± 0.0083 | 11.227 ± 0.019 | 1.209 |
| z | 0.5276 ± 0.0079 | 0.5268 ± 0.0115 | 11.040 ± 0.034 | 0.803 |

Table 4. Calculated distance of AT Vir.

| *Filter* | *Extinction* | *m* | *M* | *Distance (pc)* |
|---|---|---|---|---|
| V | 0.097 | 11.266 | 0.741 | 1339 ± 110 |
| i' | 0.067 | 11.227 | 0.638 | 1390 ± 51 |
| z | 0.048 | 11.04 | 0.665 | 1265 ± 49 |
| Average | | | | 1331 ± 41 |

Table 5. Calculated period, middle magnitude, and amplitude of HY Com.

| | *Period Calculations* | | | |
|---|---|---|---|---|
| *Filter* | *PDM* | *SL* | *Middle Magnitude* | *Amplitude* |
| B | 0.4491 ± 0.0044 | 0.4485 ± 0.005 | 10.846 ± 0.038 | 0.702 |
| V | 0.4492 ± 0.0039 | 0.4492 ± 0.0049 | 10.550 ± 0.032 | 0.474 |
| i' | 0.4491 ± 0.0048 | 0.4485 ± 0.005 | 10.395 ± 0.015 | 0.330 |
| z | 0.4491 ± 0.0042 | 0.4491 ± 0.005 | 10.215 ± 0.070 | 0.319 |

Table 6. Calculated distance of HY Com.

| *Filter* | *Extinction* | *m* | *M* | *Distance (pc)* |
|---|---|---|---|---|
| V | 0.073 | 10.55 | 0.616 | 965 ± 39 |
| i' | 0.05 | 10.365 | 0.477 | 971 ± 90 |
| z | 0.036 | 10.215 | 0.492 | 935 ± 49 |
| Average | | | | 957 ± 49 |

Table 7. Calculated period, middle magnitude, and amplitude of AE Leo.

| | *Period Calculations* | | | |
|---|---|---|---|---|
| *Filter* | *PDM* | *SL* | *Middle Magnitude* | *Amplitude* |
| B | 0.6295 ± 0.022 | 0.6261 ± 0.0225 | 12.920 ± 0.034 | 1.391 |
| V | 0.6327 ± 0.0188 | 0.6282 ± 0.0198 | 12.498 ± 0.025 | 1.235 |
| i' | 0.6295 ± 0.0214 | 0.6366 ± 0.0221 | 12.719 ± 0.030 | 0.674 |
| z | 0.6295 ± 0.0256 | 0.6295 ± 0.0256 | 12.166 ± 0.088 | 0.626 |

Table 8. Calculated distance of AE Leo.

| FilterExtinction | | m | M | Distance (pc) |
|---|---|---|---|---|
| V | 0.062 | 12.5 | 0.56 | 2372 ± 107 |
| i' | 0.042 | 12.93 | 0.4 | 2856 ± 131 |
| z | 0.031 | 12.17 | 0.41 | 2213 ± 76 |
| Average | | | | 2480 ± 76 |

The near-infrared z-band will be the most susceptible to these sorts of variations, being near a water vapor band, which accounts for that filter generally having larger error bars.

In Table 9 we present a summary of our average distances for each star computed from a straight arithmetic mean of the per-filter results. Gaia distances computed from parallaxes, a difference, and relative difference are also presented. The relative difference is the ratio of the absolute difference to the uncertainty in our average value and represents a goodness-of-match and overall are less than 2 in the worst cases. Our comparisons are done to a simple $\varpi$ distance calculation as well as to the distance results from a more comprehensive study by Bailer-Jones *et al.* (2021) that includes direction-dependent priors and various color-magnitude corrections. Our results are, on average, better fits to these.

## 4. Discussion

Overall the errors in our period calculations are less than 2%—calculated by taking the full-width-at-halfmax of the first peak in the graphs in Figures 1, 3, and 5—and therefore only affects

Table 9. Distance comparisons—differences and relative differences.

| | *AT Vir* | *HY Com* | *AE Leo* |
|---|---|---|---|
| This study | 1331 ± 41 | 957 ± 49 | 2480 ± 76 |
| Gaia (1 / [omega]) | 1319 ± 70 | 1040 ± 20 | 2698 ± 137 |
| Δr | 12 | 83 | 218 |
| Δr / max(σ) | 0.2 | 1.7 | 1.6 |
| Gaia (bj) | 1251 ± 66 | 1012 ± 17 | 2516 ± 115 |
| Δr | 80 | 55 | 36 |
| Δr / max(σ) | 1.2 | 1.1 | 0.3 |

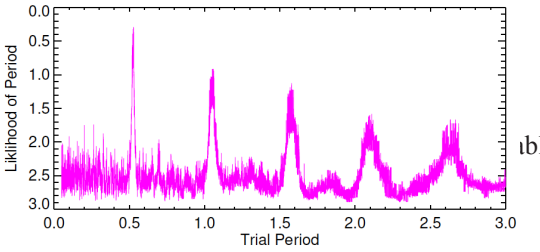


Figure 1. Period likelihood of AT Vir.

ıble 10 below presents a comparison of our calculated periods to those calculated in other studies. We found that the period we calculated is equivalent within our uncertainties. Note that the error on the literature average is a simple standard deviation of the values found and makes no attempt to weight them based on their reported uncertainties.

Interstellar reddening and extinction values found in the literature had as much as a 5% error, and thus accounted for an error in our distance calculation of approximately 0.2%. Because of how small this uncertainty is compared to those of the apparent and absolute magnitude, we conclude that reddening most likely did not play a large a role in the final uncertainty of our distance measurement. The larger concern with the reddening used is how appropriate the particular values we had found are for our study. We see in other similar studies that the value found in literature for reddening for other RR Lyrae stars has proved to be a very important issue as it is not well known (Uzpen and Slater 2020).

Another error that is cause for high uncertainty is that of the average magnitude from our light curves. In our study we found the error in the measurement for the middle magnitude to be as great as 1%, which in return is cause for as great as 5% uncertainty in the final distance. To limit this error, time was spent to obtain exposure times that would produce observations that did not collect too little or too much light from our source; we still found that some of our images were too dim and therefore unable to be used. To limit the error in the apparent magnitude of our star within our light curve, we chose to have astrosource only use 90% of our images when calculating our period and producing our light curves. Although discarding 10% of our images proved to produce viable results for HY Com and AT Vir, we found that for AE Leo, some of our images not only came back too dim, but also some had too few comparison stars, and therefore we discarded 20% of the returned images so we could produce better light curves and mitigate the error in the measured apparent magnitude. Because of this, we can see in our light curves, as shown in Figures 2, 4, and 6, that the curve is not filled out completely; this is especially the case with AT Vir and AE Leo, our RRab type stars, where there is little information on our light curves during the sharp increase in magnitude.

Being that the observations of our star were only carried out throughout the duration of approximately 20 days, it is reasonable to assume that if more images were collected over

Table 10. Period comparisons.

| | *AT Vir* | *HY Com* | *AE Leo* |
|---|---|---|---|
| This Work | 0.52359 ± 0.00854 | 0.44898 ± 0.00472 | 0.63021 ± 0.02218 |
| Kafka 2021 (AAVSO) | 0.52577 | 0.44859 | 0.62667 |
| Samus *et al.* 2017 (GCVS) | 0.52579 | — | 0.62672 |
| Alfonso-Garzón *et al.* (2012) | 0.52578 | — | — |
| Kovács (2005) | 0.52578 | — | — |
| Kunder *et al.* (2010) | 0.52979 | — | — |
| Bramich *et al.* (2014) | — | — | 0.62672 |
| Percy and Tan (2013) | — | 0.449 | — |
| Wils (2008) | — | 0.44862 | — |
| Literature Average | 0.52658 ± 0.0018 | 0.44874 ± 0.0002 | 0.62671 ± 0.0001 |
| ΔP | 0.00299 | 0.00024 | 0.0035 |
| ΔP / σ | 0.4 | 0.05 | 0.2 |

*Note: For relative differences, σ used is from this work.*

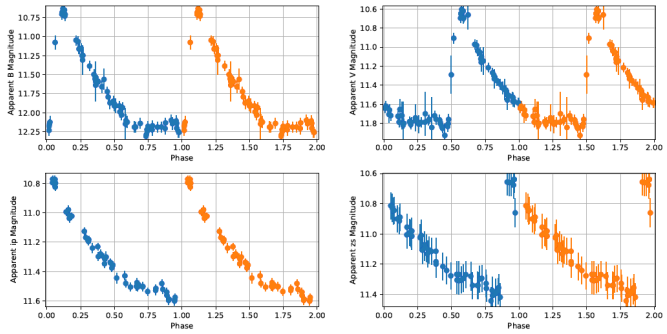


Figure 2. Phased light curves of AT Vir in B, V , i', and z filters respectively from left to right, top to bottom. A sharp peak can be seen for each curve, which is a quality known to be seen in RRab type stars.

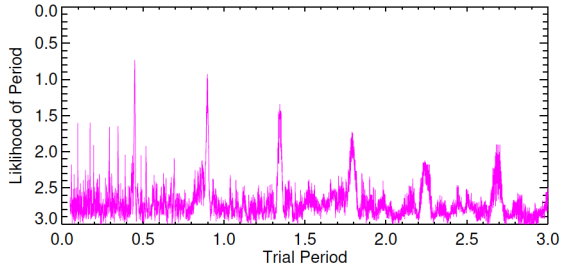


Figure 3. Period likelihood of HY Com.

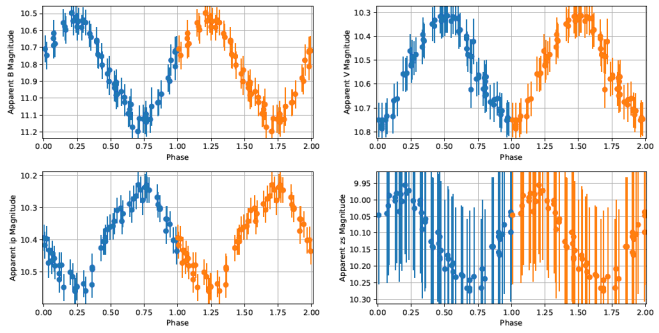


Figure 4. Phased light curves of HY Com in B, V , i', and z filters respectively from left to right, top to bottom. A more sinusoidal curve can be seen for this RRc type star.

a larger period of time, errors in apparent magnitude and period of our star would be reduced. This would allow a light curve of greater quality to be produced as more images can be taken during the sharp increase in magnitude portion of the phase of RRab type stars. Because of this loss, the apparent magnitude used in our study is the average between the minimum and maximum magnitude in effort to mitigate our uncertainty—taking the average of the entire light curve would be biased due to missing information.

It is worth noting that the overall errors for AT Vir and HY Com are comparable between our study, the simple $\varpi$ method, and the Bailer-Jones *et al.* (2021) method. Similarly, all methods have the highest errors for AE Leo; this makes sense as it is the farthest, and dimmest, of the three stars and it exhibits the Blazhko effect (Szabó 2014) that causes the amplitude of the variability to vary. In our work we have assumed this will not affect the overall calculation of the middle-magnitude "average", but it does add more noise.

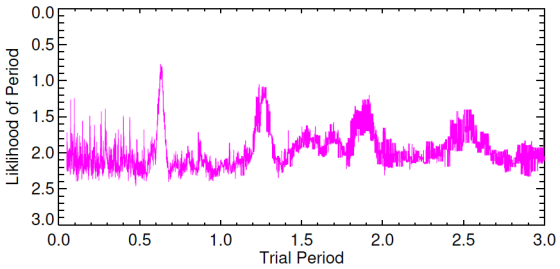


Figure 5. Period likelihood of AE Leo.

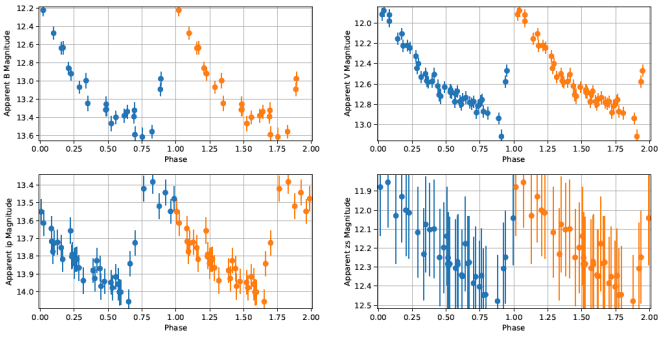


Figure 6. Phased light curves of AE Leo in B, V , i', and z filters respectively from left to right, top to bottom. Notice the light curve for this RRab type star is not as tight as that of AT Vir due to the Blazhko effect (Szabó, 2014; Layden, 1997). In this study the Blazhko effect can be ignored as only the amplitude changes while the middle magnitude is relatively constant.

## 5. Conclusion

Our work has determined the periods of AT Vir, HY Com, and AE Leo to be 0.524 ± 0.008, 0.449 ± 0.005, and 0.630 ± 0.022 day, respectively. Distances using PLM relationships (Catelan *et al.* 2004; Cáceres and Catelan 2008) yielded average distances to our stars of 1331 ± 41, 957 ± 49, and 2480 ± 76 pc, respectively. These distance calculations are equivalent, within 1.2σ, to the Gaia calculated distances of Bailer-Jones *et al.* (2021). In general this appears to support the PLM relationship method.

## 6. Acknowledgements

This work has made use of data from the AAVSO Photometric All Sky Survey (APASS; Henden *et al.* 2016).

This work has made use of data from the European Space Agency (ESA) mission Gaia (https://www.cosmos.esa.int/gaia), processed by the Gaia Data Processing and Analysis Consortium (DPAC, https://www.cosmos.esa.int/web/gaia/dpac/consortium). Funding for the DPAC has been provided by national institutions, in particular the institutions participating in the Gaia Multilateral Agreement.

This research has made use of the SIMBAD database, VizieR catalogue, and "Aladin sky atlas" developed and operated at CDS, Strasbourg, France.

We acknowledge with thanks the variable star observations from the AAVSO International Database contributed by observers worldwide and used in this research.

This research has made use of the NASA/IPAC Infrared Science Archive, which is funded by the National Aeronautics

and Space Administration and operated by the California Institute of Technology.

We also give a special thanks to Las Cumbres Observatory global telescope network and especially the support of Michael Fitzgerald and the entire Our Solar Siblings staff without whom none of this would have been possible

**References**

Alfonso-Garzón, J., Domingo, A., Mas-Hesse, J. M., and Giménez, A. 2012, *Astron. Astrophys.*, **548**, A79.

Bailer-Jones, C. A. L., Rybizki, J., Fouesneau, M., Demleitner, M., and Andrae, R. 2021, *Astron. J.*, **161**, 147.

Bertin, E., and Arnouts, S. 1996, *Astron. Astrophys., Suppl. Ser.*, **117**, 393.

Bramich, D. M., Alsubai, K. A., Arellano Ferro, A., Parley, N. R., Collier Cameron, A., Horne, K., and West, R. G. 2014, *Inf. Bull. Var. Stars*, No. 6106, 1.

Brown, T. M., *et al.* 2013, *Publ. Astron. Soc. Pacific*, **125**, 1031.

Cáceres, C., and Catelan, M. 2008, *Astrophys. J., Suppl. Ser.*, **179**, 242.

Cardelli, J. A., Clayton, G. C., and Mathis, J. S. 1989, *Astrophys. J.*, **345**, 245.

Catelan, M., Pritzl, B. J., and Smith, H. A. 2004, *Astrophys. J., Suppl. Ser.*, **154**, 633.

Collins, K. A., Kielkopf, J. F., Stassun, K. G., and Hessman, F. V. 2017, *Astron. J.*, **153**, 77.

Crestani, J., *et al.* 2021, *Astrophys. J.*, **914**, 10.

Desai, V., Rebull, L. M., and IRSA Team. 2018, in *American Astronomical Society Meeting Abstracts*, No. 232, 214.01.

Fitzgerald, M. T. 2018, *Robotic Telesc. Student Res. Education Proc.*, **1**, 347.

Fitzgerald, M. T., Gomez, E., Salimpour, S., Singleton, J., and Wibowo, R. W. 2021, *J. Open Source Software*, **6**, 2641.

Fitzgerald, M. T., McKinnon, D. H., Danaia, L., Cutts, R., Salimpour, S., and Sacchi, M. 2018, *Robotic Telesc. Student Res. Education Proc.*, **1**, 221.

Gaia Collaboration, *et al.* 2021, *Astron. Astrophys.*, **649A**, 1.

Henden, A. A., Templeton, M., Terrell, D., Smith, T. C., Levine, S., and Welch, D. 2016, AAVSO Photometric All Sky Survey (APASS) DR9 (Henden+, 2016). VizieR Online Data Catalog, II/336.

Kafka, S. 2021, Observations from the AAVSO International Database (https://www.aavso.org).

Kovács, G. 2005, *Astron. Astrophys.*, **438**, 227.

Kunder, A., Chaboyer, B., and Layden, A. 2010, *Astron. J.*, **139**, 415.

Lafler, J., and Kinman, T. D. 1965, *Astrophys. J., Suppl. Ser.*, **11**, 216.

Layden, A. C. 1994, *Astron. J.*, **108**, 1016.

Layden, A. C. 1997, *Publ. Astron. Soc. Pacific*, **109**, 524.

Longmore, A. J., Fernley, J. A., and Jameson, R. F. 1986, *Mon. Not. Roy. Astron. Soc.*, **220**, 279.

Ochsenbein, F., Bauer, P., and Marcout, J. 2000, *Astron. Astrophys., Suppl. Ser.*, **143**, 23.

Percy, J. R., and Tan, P. J. 2013, *J. Amer. Assoc. Var. Star Obs.*, **41**, 75.

Salaris, M., Chieffi, A., and Straniero, O. 1993, *Astrophys. J.*, **414**, 580.

Samus, N. N., Kazarovets, E. V., Durlevich, O. V., Kireeva, N. N., and Pastukhova, E. N. 2017, *Astron. Rep.*, **61**, 80, *General Catalogue of Variable Stars: Version GCVS 5.1* (http://www.sai.msu.su/gcvs/gcvs/index.htm).

Schlafly, E. F., and Finkbeiner, D. P. 2011, *Astrophys. J.*, **737**, 103.

Stellingwerf, R. F. 1978, *Astrophys. J.*, **224**, 953.

Szabó, R. 2014, in *Precision Asteroseismology*, eds. J. A. Guzik, W. J. Chaplin, G. Handler, A. Pigulski, IAU Symp. 301, 241.

Uzpen, B., and Slater, T. F. 2020, *Astron. Theory Obs. Methods*, **1**, 54.

Wils, P. 2008, *Perem. Zvezdy*, **28**, 1.

Wolf, C., *et al.* 2018, *Publ. Astron. Soc. Australia*, **35**, e010.